






Uncertainty Assessment in Soil Erosion Modelling Using RUSLE, Multisource and Multiresolution DEMs

Ashish Pandey¹  · Amar Kant Gautam² · V. M. Chowdary³  · C. S. Jha⁴ · Artemi Cerdà⁵ 

Received: 10 January 2021 / Accepted: 10 March 2021 / Published online: 25 March 2021
© Indian Society of Remote Sensing 2021

Abstract

Soil erosion is a key concern for the environment and natural resources since it leads to a decline in-field productivity and soil quality, resulting in land degradation. In this study, assessment of uncertainty in soil erosion modelling of the Karso watershed, India, was carried out by employing the revised universal soil loss equation (RUSLE) and geospatial technologies to evaluate the effect of multi-source digital elevation models (DEMs) [Advanced Spaceborne Thermal Emission and Reflection Radiometer (ASTER), Cartosat and Shuttle Radar Topography Mission (SRTM)] with resampled multi-resolution grids. The rainfall erosivity factor (R) was computed using the mean monthly Tropical Rainfall Measuring Mission rainfall estimates for 1998 to 2012. The slope length factor was derived using the ASTER and Cartosat DEMs at grid sizes of 30 m, 50 m, 100 m, 150 m, 200 m, and 250 m, and for the SRTM DEM at 100 m, 150 m, 200 m and 250 m resolutions for the Karso watershed, Jharkhand, India. Significant differences were obtained in the soil loss estimates across the different DEM sources and resampled grid sizes. The Cartosat DEM with a 200 m grid was found to estimate the soil loss the best out of all the DEM combinations considered. The Cartosat DEM proved to be more reliable than the ASTER and SRTM DEMs. The results indicated that the RUSLE is a scale-dependent model since the model estimates were affected not only by the DEM source but also by its resolution. The prediction of erosion potential by employing the multisource, multiresolution DEMs and the RUSLE helped to identify the soil erosion's spatial pattern within the watershed. The study provided an impact analysis of the uncertainties when selecting the multisource, multiresolution DEMs for soil erosion modelling.

Keywords ASTER · Cartosat · Grid size · TRMM · Soil erosion · SRTM

✉ Ashish Pandey
ashish.pandey@wr.iitr.ac.in

Amar Kant Gautam
agautam@wr.iitr.ac.in

V. M. Chowdary
chowdary_isro@yahoo.com

C. S. Jha
jha_cs@nrsc.gov.in

Artemi Cerdà
artemio.cerda@uv.es

² Dr. Rajendra Prasad Central Agricultural University,
Pusa, Samastipur, Bihar 848125, India

³ RRSC-North, National Remote Sensing Centre (NRSC),
Indian Space Research Organization, Delhi, India

⁴ Regional Remote Sensing Centres, National Remote Sensing
Centre (NRSC), Indian Space Research Organization,
Hyderabad, India

⁵ Departament de Geografia, Universitat de València, Blasco
Ibáñez, 28, 46010 Valencia, Spain

¹ Department of Water Resources Development and
Management, Indian Institute of Technology Roorkee,
Roorkee, India

Introduction

Soil erosion is a severe environmental problem in developing countries (Keesstra et al. 2018a, b; Rodrigo-Comino 2018; Wuepper et al. 2020). Soil losses are no sustainable in agricultural lands such as vineyards (López-Vicente et al. 2020; Rodrigo-Comino et al. 2018), citrus (Keesstra et al. 2019), Persimmon (Cerdà et al. 2017), and olive plantations (Rodrigo-Comino et al. 2020) and also in forest land due to forest fires and grazing (Alcañiz et al. 2020; Cerdà et al. 2020). Soil erosion induces the loss of organic matter, soil compaction, and soil biodiversity loss, resulting in reduced soil quality and soil fertility, influencing land degradation processes (Novara et al. 2019).

In India, about 5334 m-tonnes of soil is being detached annually due to various reasons and its rate is about $16.40 \text{ Mg ha}^{-1} \text{ year}^{-1}$ (Narayana 1983). Erosion levels are high in Asia, Africa and South America, where its rate varies from 30 to $40 \text{ Mg ha}^{-1} \text{ year}^{-1}$ (Barrow 1991). Erosion leads to loss of the topsoil that provides water- and nutrient-holding capacity (Keesstra et al. 2018a, b).

Several soil erosion studies have been carried out by several researchers (Chen et al. 2011; Demirci and Karaburun 2012; Ghosal and Bhattacharya 2020; Pandey et al. 2007) using geospatial technologies. Thomas et al. (2018) modelled soil erosion and deposition in a tropical mountainous river basin in a rain shadow region of the southern Western Ghats (India) using RUSLE and the transport-limited sediment delivery function in GIS. A DEM is a quantitative representation of the terrain relief and is one of the most important spatial data sources for hydrological modelling (deVente et al. 2009). The increased availability of DEMs from different sources at global and regional scales offers new opportunities to apply models for various environmental applications (Li and Wong 2010; Lin et al. 2013). DEMs with higher accuracy were used by various researchers (Prasuhn et al. 2013; Quiquerez et al. 2014) to improve soil erosion estimation accuracy. In recent years, multiresolution DEMs, namely (1) ASTER (Advanced Spaceborne Thermal Emission and Reflection Radiometer) at 30 m, (2) Cartosat-1 at 30 m, and (3) SRTM (Shuttle Radar Topography Mission) at 90 m resolutions, are freely available in the web. Hence, the data availability problem about terrain relief, one of the most critical parameters for soil erosion modelling (Wechsler 2007), has become less important. However, uncertainties do exist in the DEM and are rarely accounted in hydrological studies (Datta and Schack-Kirchner 2010). The DEM source and resolution affect the accuracy of the extracted topographical parameters (Sharma et al. 2011). The arbitrary choice of grid resolution for the contour-derived DEM is one of the major sources of uncertainty in

the hydrological modelling process (Zhang et al. 2008). The uncertainty associated with DEM-derived topographic parameters can reduce the reliability of the modelled erosion estimates (Sharma et al. 2011). DEMs are affected by the delineation of hill slopes and channel systems, leading to discrepancies in the erosion estimates (Walker and Willgoose 1999). Thus, the selection of the DEM is vital for environmental applications (Li and Wong 2010).

Furthermore, the functional relationship between the effect of the grid size and the sediment yield modelling was studied by various researchers using different empirical, conceptual and physical models (Chaubey et al. 2005; Cochrane and Flanagan 2005; Cotter et al. 2003; Lin et al. 2010; Renschler and Harbor 2002). Molnár and Julien (1998) reported that the USLE model underestimated the soil loss with increased grid size. Wu et al. (2005) and Nikolakopoulos et al. (2006) also reported that the grid size effect on a USLE-based soil estimate is significant. deVente et al. (2009) used a USLE-based soil loss model called WATEM–SEDEM to illustrate ASTER and SRTM DEMs' effect on sediment yield.

Researchers have evaluated relevant topographic parameters derived from different DEMs for accuracy assessment (Ahmed et al. 2007; Hancock et al. 2006; Hayakawa et al. 2008; Hirt et al. 2010; Mukherjee et al. 2013; Muralikrishnan et al. 2013). deVente et al. (2009) reported that the SRTM DEM provides more accurate estimates of the slope gradient and upslope drainage area than the ASTER DEM. Hancock et al. (2006) recommended the SRTM DEM for the qualitative assessment of large catchments. They found that calibrated sediment transport parameters were almost five times higher with a 10 m DEM than with the 90 m SRTM DEM. Käab (2005) reported that the SRTM DEM is better than the ASTER DEM. Thus, the uncertainties associated with the DEM-derived topographical parameters for soil erosion modelling can reduce the predicted erosion estimates' reliability. Several researchers used the spatially distributed erosion model RUSLE to assess annual soil erosion estimates due to the effect of water (Van Oost et al. 2000; Van Rompaey et al. 2001).

The justification for employing a particular grid size in a DEM lacks in most of the relevant literature. However, researchers have suggested that the DEM size should be selected appropriately to reflect spatial variations (Nikolakopoulos et al. 2006) adequately. Topographical parameters, namely the slope and slope length (LS) factor, are essential for erosion modelling, computed using multi-source and multiresolution DEMs. Therefore, the present study was carried out with the objective to assess the uncertainty in soil erosion modelling using the revised universal soil loss equation (RUSLE), multisource and multiresolution DEMs (SRTM, ASTER and Cartosat).

Study Area

The study area, Karso watershed, is a part of the Damodar–Barakar catchment and is geographically located between 85°23' to 85°28'E longitude and 24°12' to 24°18'N latitude (Fig. 1). The total area of this watershed is approximately 28 km². The average annual rainfall in this watershed is nearly 1300 mm and 75% of the total annual rainfall occurs during the monsoon season (June to October) (Pandey et al. 2008). The minimum and maximum temperatures vary from 3 to 42 °C. The main soil textural class is sandy loam and its depth varies from 0 to 45 cm (Pandey et al. 2008). The majority of the watershed's land slope ranges between 0 and 8%, while the highest slope up to 22% is observed in some parts of the watershed. Paddy is the dominant crop in the study area.

Methodology

The soil erosion modelling for the case study area was carried out using the RUSLE model, while the model parameters were derived using remote sensing and GIS technologies. One of the important parameters of the soil erosion model, i.e., the LS factor, was derived using multisource, multiresolution DEMs (SRTM, ASTER and Cartosat-Dem). The methodology flowchart for the estimation of the soil loss is given in Fig. 2.

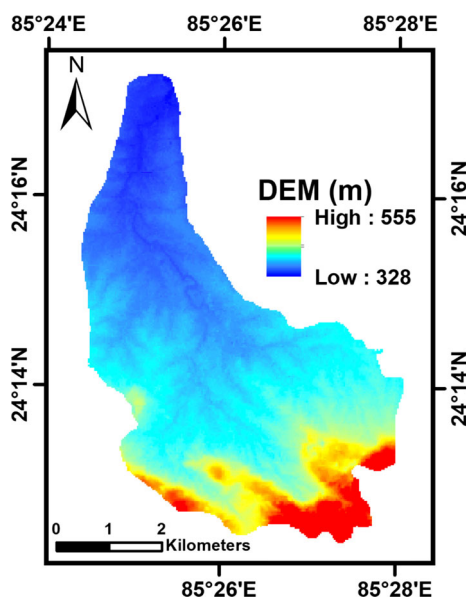


Fig. 1 Map of the study area. DEM digital elevation model

Erosion Modelling Using the RUSLE

The application of the RUSLE in the grid environment with GIS helped us to model the soil erosion process in a spatially distributed manner. This model is a simple multiplicative model and is widely reported in the literature (Angima et al. 2003; Pandey et al. 2008). The average annual soil loss was estimated using the following equation:

$$A = R \times K \times LS \times C \times P \quad (1)$$

where A is the annual soil loss per unit area (Mg ha year⁻¹), R is the rainfall erosive factor (MJ mm ha⁻¹ h⁻¹ year⁻¹), K is the soil erodibility factor (Mg h MJ⁻¹ mm⁻¹), LS is the dimensionless slope length factor, C is a dimensionless land cover and management or cropping factor and P is a dimensionless conservation practice factor. Analogous to the DEM, all RUSLE input layers, i.e., the R , K , C , and P factors, were prepared at different grid resolutions, namely 30 m, 50 m, 100 m, 150 m, 200 m, and 250 m, for assessing the soil erosion at different resolutions.

Rainfall Erosivity Factor (R)

The R factor is the product of the total storm kinetic energy (E) and the maximum 30 min rainfall intensity (I_{30}) (Renard et al. 1997). In general, the monthly, seasonal, and annual rainfall statistics are usually available from nearby hydrological or meteorological stations and are used as a substitute for EI_{30} when estimating the rainfall erosivity. To overcome the absence of rain gauge stations in the study area, remotely sensed Tropical Rainfall Measuring Mission (TRMM) data was used to compute the rainfall erosivity factor. Satellite-based precipitation data are especially useful in semi-arid regions, where ground measurements are scarce or not present (Katiraie-Boroujerdy et al. 2013). The TRMM data has been available since 1997 (Kummerow et al. 1998).

Various researchers have reported that the TRMM-derived rainfall is well correlated with the ground-based precipitation measurements (Collischonn et al. 2008; Karaseva et al. 2011; Islam et al. 2007; Duncan and Biggs 2012). Particularly, in developing countries, the availability of continuous long-term rainfall data records is scarce (Cohen et al. 2005; Diodato et al. 2007; Shamshad et al. 2008). Hence, in this study, TRMM rainfall that was archived from <http://disc.sci.gsfc.nasa.gov/precipitation/tovas/> was used. Vrieling et al. (2008) and Vrieling et al. (2010) utilized the TRMM rainfall data for estimating the average annual R factor in their studies. Thus, for assessing the R factor, the relationship between the annual rainfall and the EI_{30} values proposed by Singh et al. (1981) for

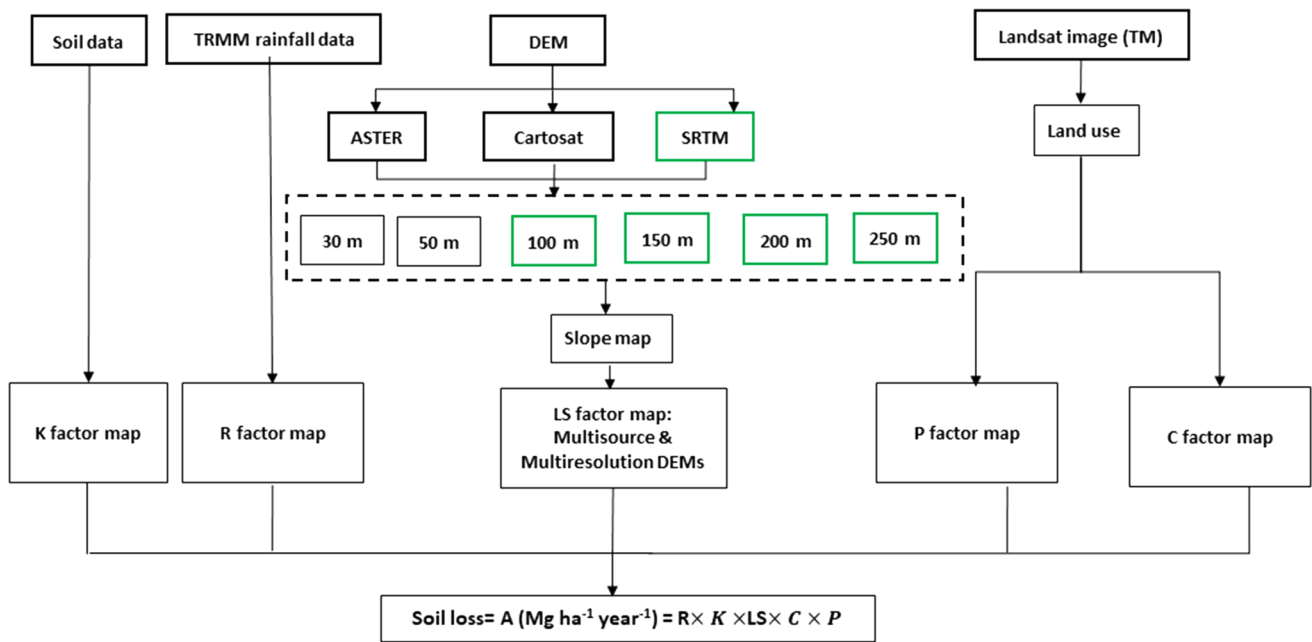


Fig. 2 Methodology flowchart for the estimation of soil loss. *ASTER* Advanced Spaceborne Thermal Emission and Reflection Radiometer, *SRTM* Shuttle Radar Topography Mission, *TM* Thematic Mapper, *TRMM* Tropical Rainfall Measuring Mission

different climatic zones of India was used. Mean monthly rainfall data extracted from the TRMM rainfall grid for the period 1998–2012 was used for computation of R factor as given below:

$$R = 79 + 0.363P_n \quad (2)$$

where R is the rainfall erosivity factor ($\text{MJ mm ha}^{-1} \text{ h}^{-1} \text{ year}^{-1}$) and P_n is average annual rainfall (mm).

Soil Erodibility Factor (K)

The K factor was computed using the following relationship:

$$K = 2.8 \times 10^{-7} \times M^{1.14} \times (12 - a) + 4.3 \times 10^{-3} \times (b - 2) + 10^{-3} \times (c - 3) \quad (3)$$

where M is the particle size parameter = (percent silt + percent very fine sand) (100 – percent clay), a is the percentage of organic matter, b is the soil structure code used in soil classification and c is the soil permeability class. The soil erodibility factor (K) computed by (Pandey et al. 2007) was adopted in this study.

Slope Length Factor (LS Factor)

Topography affects the runoff and transport processes of sediment at the watershed scale (Pandey et al. 2007). The LS factor, the combined slope length and the slope steepness factor are some of the most important inputs for the

RUSLE model and were computed for multi-resolution and multi-source DEMs. The LS factor characterizes the effect of topography and hydrology on the soil loss. Soil loss estimates are more sensitive to the slope steepness than the slope length (Nikolakopoulos et al. 2006). The LS factor was computed in GIS using the relationship proposed by (Moore and Burch 1986), which is given as follows:

$$LS = \left[\frac{\lambda}{22.13} \right]^m \left[\frac{\sin \alpha}{0.0896} \right]^n \quad (3)$$

where λ is the field slope length (m), and α is the slope gradient in degrees. The value of m depends on the slope steepness value: 0.5 for slopes exceeding 5%, 0.4 for 4% slopes, and 0.3 for slopes less than 3% and the value of n is 1.3. Several researchers computed the LS factor using Eq. (4) with similar assumptions (Fistikoglu and Harmancioglu 2002; Onyando et al. 2005; Pandey et al. 2007). Further, the effect of LS factor on the RUSLE model estimates derived using multiple DEM grid sizes was studied and compared to the observed soil loss data for the period 1998–2001. The SRTM, ASTER and Cartosat-1 DEMs that were available at 90, 30 and 30 m resolutions, respectively, were resampled to multiple grid resolutions (50, 100, 150, 200 and 250 m) using bilinear interpolation techniques in ESRI ARC-GIS 10.2 for extraction of the LS parameters that are important for regional erosion modelling.

Crop Management Factor (C-Factor)

The *C* factor in the RUSLE model represents the crop/vegetation in the study area. Cloud-free digital data from the Landsat TM satellite (30 m spatial resolution) acquired from <http://glovis.usgs.gov/> was used for generation of the land-use/land-cover map of the study area. Ground truth collected during field visits and information from Google Earth were used for the supervised classification of the satellite data using digital image processing software.

The classified images depicting the various land-use/land-cover classes of the study area derived from the digital interpretation of the satellite imagery were used for assigning a crop management factor (*C*-factor) to each land-use/land-cover class. A *C*-factor of 0.28 was assigned to agriculture and paddy fields based on the previous studies carried out in different parts of India (Dabral et al. 2008; Pandey et al. 2009; Rao 1981).

Conservation Practices Factor (P-Factor)

The RUSLE conservation practices factor (*P*-factor) was assumed to be 0.28 for agricultural lands (paddy and upland cultivation), as mostly cultivation is done using banded fields, while the value of 1 was assigned to other land-use/land-cover classes as suggested by (Mondal et al. 2017; Pandey et al. 2007).

Multisource, Multiresolution DEMs

ASTER DEM

The ASTER has three spectral bands in the visible near-infrared (VNIR), six bands in the shortwave infrared (SWIR), and five bands in the tier regions (Yamaguchi et al. 1998). The ASTER DEM with a 30 m resolution was downloaded from <http://gdem.ersdac.jspacesystems.or.jp/>.

Cartosat-1 DEM

The Cartosat DEM was obtained from BHUVAN-ISRO's Geoportal/Gateway to the Indian Earth Observation <http://bhuvan-noeda.nrsc.gov.in>. (Hancock et al. 2006) reported that the DEM produced from the Cartosat 1 stereo pair is suitable for operational use in planning and is better than the other publicly available DEMs, such as the SRTM and ASTER DEMs. The depression-less DEM was used for generating the relevant parameters for erosion modelling. The planimetric and vertical accuracies of the national-level Carto DEM were 15 m (CEP 90) and 8 m (LE90) (Murthy et al. 2008).

SRTM DEM The SRTM dataset is freely available from <http://srtm.csi.cgiar.org/>. Various researchers have reported (Rabus et al. 2003) a vertical accuracy of 16 m, a horizontal positional accuracy of 20 m, and a relative vertical accuracy of 6 m for the SRTM-1 DEM. A comparison between ASTER, Cartosat-1 and SRTM DEMs elevations in the study area is presented in Table 1.

Validation of the RUSLE Model Soil Erosion Estimates

For the validation of the RUSLE model estimates, the sensitivity analysis of the *LS* factor derived from multi-source DEMs was carried out using the observed sediment yield data for the period 1998–2001 from the Damodar Valley Corporation (DVC), Hazaribagh. The annual soil loss was estimated by summing up the measured soil loss of all individual rainfall events measured for all the rainfall events in a particular year for 1998–2001. Subsequently, the annual soil loss in Mg ha^{-1} was obtained by dividing the total annual sediment in tonnes by the total area of the watershed. The sediment concentration was considered to be 1.4 g/cm^3 in this study.

Results

Spatial Inputs for the Erosion Modelling using the RUSLE

The rainfall erosivity factors were computed for each year using the TRMM rainfall data for 1998–2012 (Table 2). The spatial distribution of the soil erodibility factor ($\text{Mg ha h ha}^{-1} \text{ MJ}^{-1} \text{ mm}^{-1}$) is given in Fig. 3a.

The spatial distribution of eight different land-use/land-cover classes in the watershed and its area statistics are given in Fig. 1b and Table 3, respectively. The error matrix that indicates the accuracy of the supervised classification is given in Table 4. The estimated accuracy based on 477 random samples representing various land-use/land-cover categories exhibited an overall accuracy of 77.36%. The kappa coefficient (κ), which was originally developed to measure the observer agreement for categorical data (Cohen 1968), was estimated to be 0.73. The *C*-factor and *P*-factor for different land-use/land-cover classes is presented in Table 5. The magnitude and the spatial distribution of the *C*-factor and *P*-factor are presented in Fig. 1c–d.

In this study, RUSLE model was used to assess the uncertainties in soil loss of the Karso watershed using the TRMM-derived *R* and *LS* factors from multi-source DEMs (ASTER DEM, Cartosat DEM and SRTM DEM) with multi-grid resolutions. Variations in the minimum and

Table 1 Comparison between the ASTER, Cartosat-1 and SRTM DEMs elevations

DEM source	Generation and distribution	Data acquisition period	Minimum elevation (m)	Maximum elevation (m)	Average (m)	SD
ASTER	METI/NASA	February 2000 (Fujisada et al. 2005)	378	657	384.67	40.96
Cartosat-1	NRSC/ISRO	May 05, 2005 (Muralikrishnan et al. 2013)	327	555	434.33	50.18
SRTM	NASA/USGS	February 11–22, 2000 (Hayakawa et al. 2008)	385	665	442.46	48.65

Table 2 Estimation of the rainfall erosivity factor using the TRMM data

Year	<i>R</i> factor	Year	<i>R</i> factor
1998	635.22	2006	577.33
1999	632.41	2007	656.1
2000	498.78	2008	567.21
2001	498.07	2009	413.82
2002	480.48	2010	416.36
2003	540.54	2011	635.72
2004	499.92	2012	525.03
2005	410.54	–	–

maximum elevations between the three DEMs are evident in Table 1. The minimum and maximum elevations for ASTER and SRTM were nearly the same; conversely, the average elevation was nearly the same for SRTM and Cartosat. The mean elevation of the ASTER DEM was lower than the SRTM and Cartosat-DEM by 58 m and 50 m, respectively. LS factor's mean and maximum values were derived using ASTER, Cartosat and SRTM DEMs for different grid resolutions (Table 6 and Fig. 4), where the slope length factor (LS) is the most relevant parameter for erosion modelling. The spatial distribution of these LS factors computed for different combinations of DEM and grid resolution is presented in Fig. 5a–c. The Cartosat-DEM-based LS factors had the lowest mean and maximum values, while the ASTER and SRTM DEMs produced higher LS values (Table 6). For ASTER DEM, the maximum value of the slope length factor increased as the DEMs were resampled from 50 to 100 m grid sizes, and this value decreased with the increase in the grid sizes from 150 to 250 m. However, a similar trend was observed in case of the Cartosat and SRTM DEMs, but the changes were more prominent for ASTER DEM, which could be attributed to the averaging effect due to increased grid sizes.

Furthermore, it was observed that the averaging effect was more in case of ASTER DEM that likely influenced the spatial patterns and magnitude of the sediment sources and sinks. The resampling of DEM resolutions also greatly affected the distribution of the slopes, and subsequently, on the channel network and slope length factors. Sharma et al. (2011) and Nikolakopoulos et al. (2006) also reported that the LS factor decreased with the increase in DEM grid size.

Evaluation of the Grid Size on the Soil Erosion Estimates

Soil erosion from the Karso watershed was estimated using the RUSLE model with multi-resolution grid parameters derived from multi-source DEMs and the TRMM-based rainfall erosivity factor (*R*) during the period 2002–2012. The percentage deviation of the RUSLE erosion estimates for the period 1998–2001 varied from 1.85 to 16.99%; we found that the soil loss computed using the 200 m Cartosat-DEM-derived parameters for multiple grid resolutions was close to the observed sediment yield, except for the 250 m grid. (Table 7). The spatial distribution of the average annual soil loss estimated using the ASTER-, Cartosat- and SRTM-derived parameters is presented in Fig. 6a–c.

Furthermore, the soil losses computed for the period 1998–2012 are presented in Table 8. The estimated soil loss of the watershed varied for different source DEMs from the highest [9.87 Mg ha⁻¹, ASTER (30 m)] to lowest [2.19 Mg ha⁻¹, Cartosat (200 m)] for the years 1998 to 2012 (Table 8). It can be seen from Table 8 that the computed soil losses using the ASTER-DEM-based parameters were found to be the most overestimated, followed by the SRTM-DEM-derived parameters. The percentage variation in the soil loss estimates for different grid resolutions in the case of the Carto DEM was marginal, while it was prominent in the ASTER DEM case (Table 8).

The resampling of the ASTER DEM from 30 m resulted in a decrease in the average annual soil loss by 6.16%, while it decreased by 2.22% for the Carto DEM. The

Fig. 3 **a** Spatial distribution of the soil erodibility factor, **b** classified land-use/land-cover map, **c** spatial distribution of the crop management (*C*) factor, **d** spatial distribution of the conservation management factor (*P*) factor

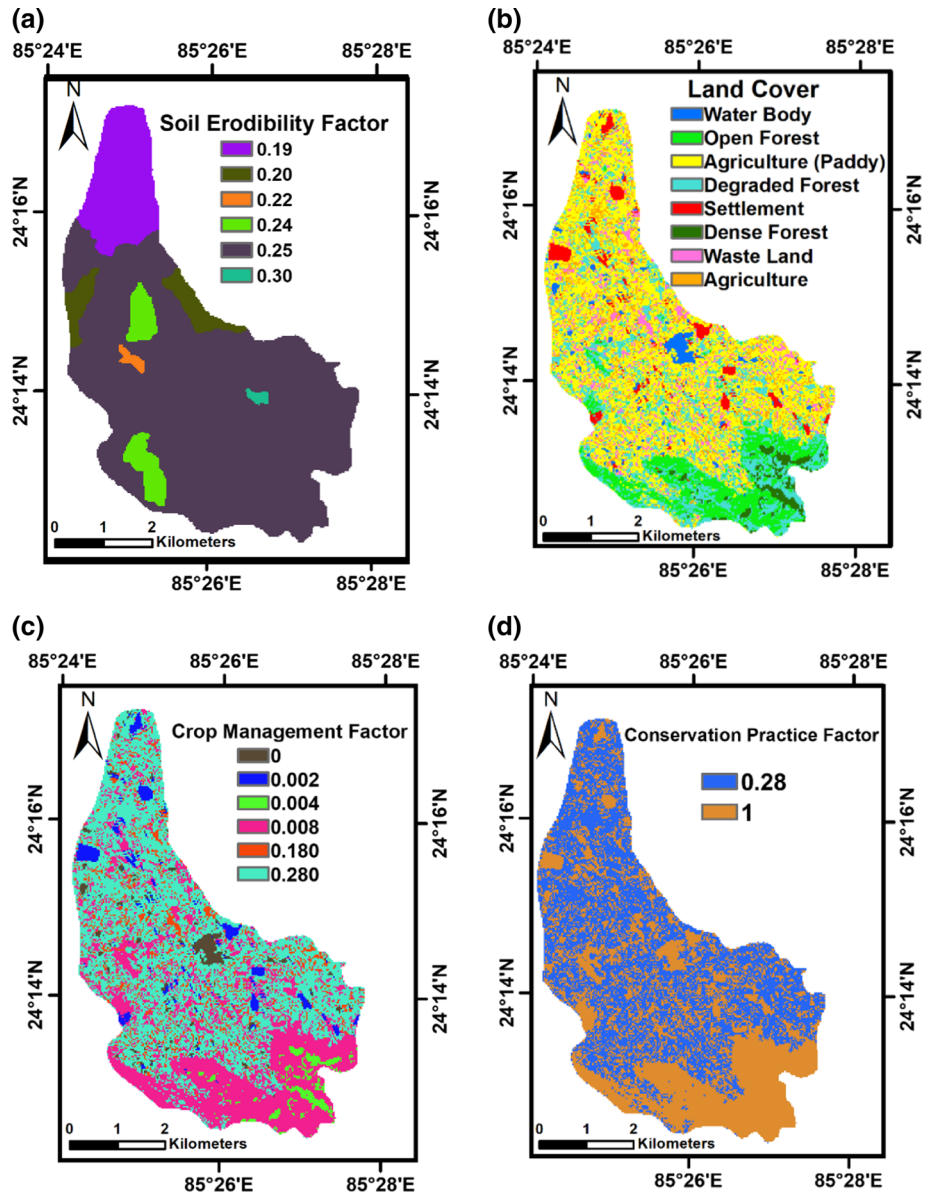


Table 3 Land-use/land-cover statistics of the Karso watershed

Land use/land cover	Area (ha)	Area (%)
Water body	76.5	2.74
Open forest	293.31	10.5
Paddy	1210.77	43.35
Degraded forest	605.88	21.69
Settlement	98.01	3.51
Dense forest	60.3	2.16
Wasteland	226.08	8.09
Agriculture (upland crop)	222.21	7.96
Total	2793.06	100

decrease in soil loss with an increase in DEM resolution was reported by many researchers (Cho and Lee 2001; Di Luzio et al. 2004; Molnár and Julien 1998; Nikolakopoulos et al. 2006). Conversely, (Verstraeten 2006) reported a higher RUSLE-based soil loss with SRTM DEM than a 20 m DEM in the Scheldt River basin. The average annual soil losses computed using topographic parameters derived from ASTER, SRTM, and Cartosat with 100 m resolution grids were found to be 5.75, 3.69 and 2.98 Mg ha⁻¹ - year⁻¹, respectively. The soil losses in the case of 150 m grid resolution was increased by 9.3% for ASTER, 6% for Cartosat and 7.5% for SRTM. The lower slope gradients that were aggregated for coarse resolution DEMs might have led to steeper slopes in low-slope categories and high-resolution DEMs were less smooth than the low-resolution

Table 4 Classification accuracy assessment

Class	W	OF	P	DGF	S	DF	WL	A	Row total	EC	EO
W	33	0	0	0	3	3	3	0	42	21.43	0.00
OF	0	57	0	0	0	0	0	0	60	5.00	26.92
P	0	6	87	9	0	0	6	12	120	27.50	14.71
DGF	0	6	6	45	0	0	0	0	60	25.00	31.82
S	0	0	0	0	30	0	12	3	45	33.33	9.09
DF	0	3	0	3	0	24	0	0	30	20.00	20.00
WL	0	6	3	0	0	0	48	3	60	20.00	33.33
A	0	0	3	9	0	0	3	45	60	25.00	28.57
Column totals	33	78	102	66	33	30	72	63	477		

Table 5 Crop management factor and conservation practice factor for different land-use/land-cover classes

Land use/land cover	C factor	P factor
Water body	0	1
Open forest	0.08	1
Paddy	0.28	0.28
Degraded forest	0.08	1
Settlement	0.02	1
Dense forest	0.04	1
Wasteland	0.18	1
Agriculture (upland Crop)	0.28	0.28

W water body, OF open forest, P paddy, DGF degraded forest, S settlement, DF dense forest, WL wasteland, A agriculture (upland crop)

Table 6 Mean and maximum LS factors for different grid sizes

Grid size (m)	ASTER		Cartosat-1		SRTM	
	Mean	Max	Max	Mean	Max	Mean
30	1.68	15.80	13.31	0.88		
50	1.70	17.78	12.47	0.90		
100	1.48	19.33	13.42	0.90	18.39	1.37
150	1.44	15.14	10.47	0.90	19.81	1.39
200	1.40	14.37	9.03	0.86	17.42	1.39
250	1.33	13.15	8.96	0.85	14.63	1.29

DEMs (Li and Wong 2010). The estimated average annual soil losses for SRTM (200 m), ASTER (200 m) and Cartosat (200 m) DEMs were 3.54, 4.53 and 2.96 Mg ha⁻¹, respectively. Compared to estimated soil loss for the grid resolution of 150 m, the soil loss decreased by 39.95% for ASTER, 7.09% for Cartosat and 12.71% for SRTM. For the grid size of 250 m, the computed average annual soil loss increased by 2.58% for ASTER, 12.16% for Cartosat (150 m) and 11.72% for SRTM. The soil loss estimate

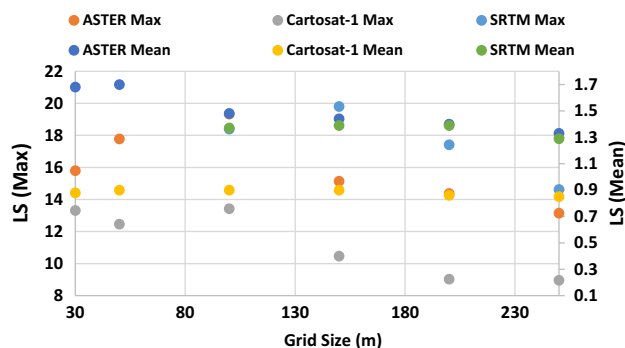


Fig. 4 Mean and maximum LS factors for different grid sizes

decreased with a coarser resampled DEM, which was consistent with (Chaubey et al. 2005).

Discussion

The RUSLE is a scale-dependent model, where the soil loss estimates observed in this study were affected not only by the DEM source but also by its resolution (Table 8). The DEM used is one of the important parameters that are likely to induce uncertainty in soil erosion estimates, along with rainfall and soil erodibility factors. In this analysis, the mean and maximum LS factors increased with an increase in the DEM resolution up to 50 m and 100 m, respectively, and subsequently decreased with an increase in the DEM resolution.

These changes were more prominent in the case of ASTER DEM. Contrary to these results, (Mondal et al. 2017) reported that the mean slope and mean LS factor decreased with increased DEM resolution in their studies carried out in the west-flowing Narmada River basin. However, they reported poor results when the ASTER DEM was used for soil erosion modelling. In this study, the predicted soil loss with ASTER DEM (30 m) was also much higher than Cartosat (30 m) for each DEM resolution. Prasuhn et al. (2013) also reported the poor performance of the ASTER DEM for soil erosion estimation in

Fig. 5 **a** Spatial distribution of the slope length factor for different grid sizes (ASTER), **b** spatial distribution of the slope length factor for different grid sizes (Cartosat-1) and **c** spatial distribution of the slope length factor for different grid sizes (SRTM)

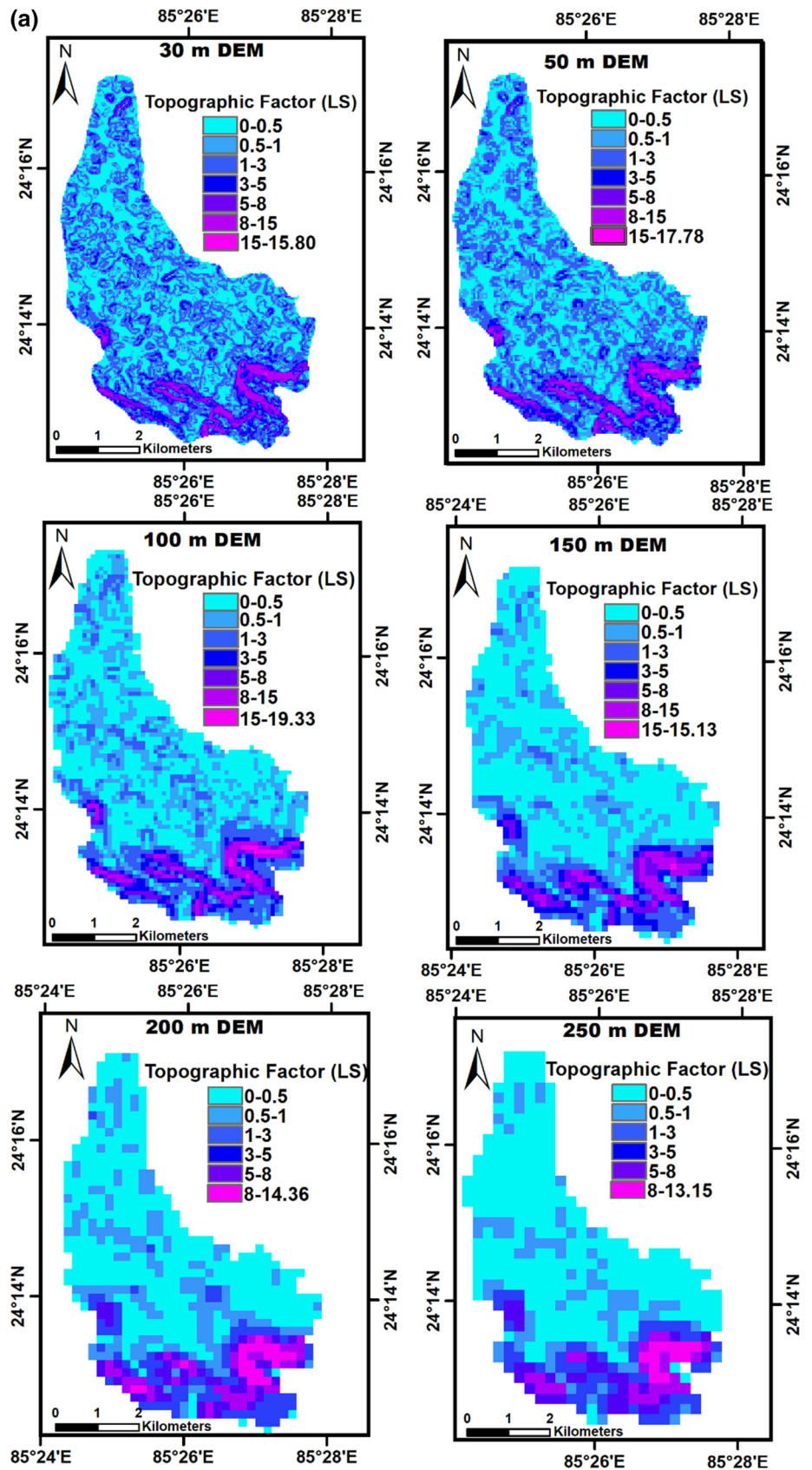


Fig. 5 continued

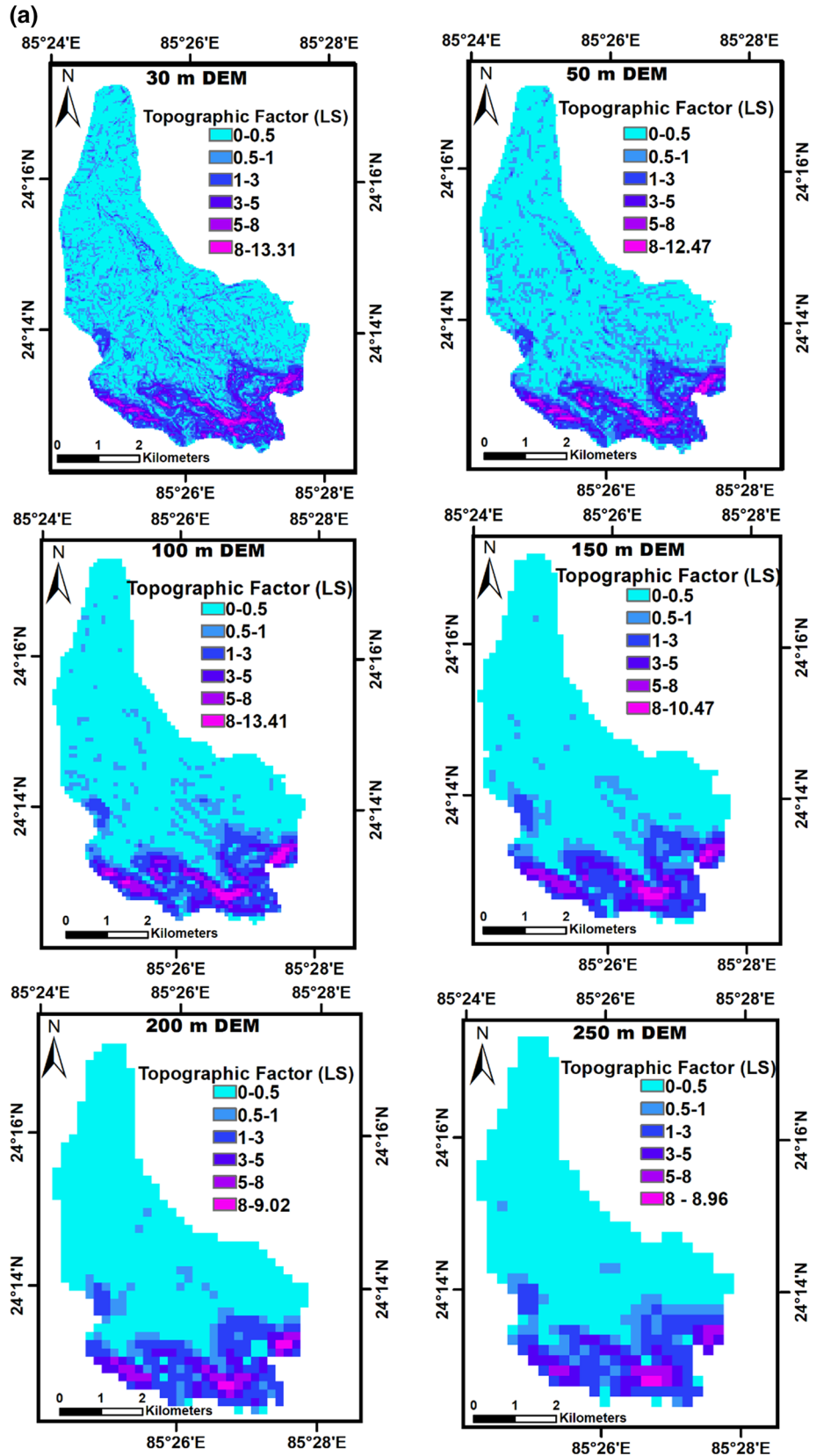
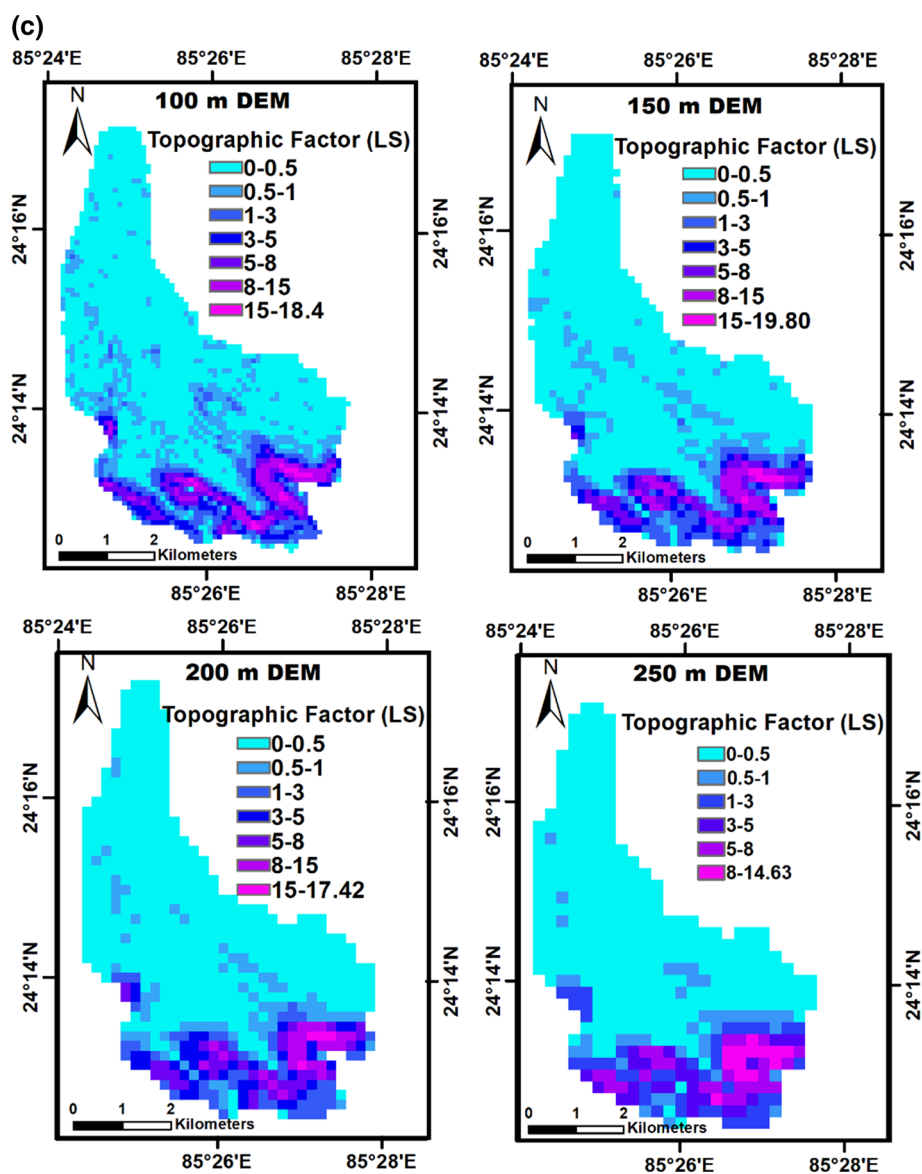


Fig. 5 continued



comparison to the SRTM DEM despite the better vertical accuracy. The Cartosat DEM at 100 m and 150 m grid sizes appear to be a threshold, where the RUSLE estimates for these grid resolutions match reasonably with the observed soil loss. In the SRTM DEM case, the parameters derived using a 200 m resolution grid yielded better estimates compared to other grid resolutions. Although the percentage deviations between the observed and simulated sediments were reduced with the increase in the ASTER DEM grid sizes from 30 to 250 m, the ASTER DEM inputs performed worst among all the DEMs, followed by the SRTM DEM. Soil erosion studies carried out by (Mondal et al. 2017) using GTOPO30, SRTM (90 m), Cartosat (30 m), ASTER and SRTM (30 m) indicated that the soil erosion results were better in the case of SRTM (30 m) and very poor in the case of GTOPO30. This observation is

consistent with Lin et al. (2013), as the SRTM-DEM-based erosion estimates were better compared with the field measurements.

Vieux and Needham (1993) reported that the grid size of 400 m appears to be a critical value, below which the channel erosion and shorter flow lengths dominate the erosion process. The flow path length response to the cell sizes is expected since the flow path meanderings are short-circuited with larger cell sizes. Channel erosion and shorter flow lengths dominate the erosion process with smaller DEM grid sizes. Thus, contrary to the general perception that a finer resolution gives better results while an increased grid size gives a generalized soil erosion estimate (Mondal et al. 2017), a distinct pattern in the LS values was shown with an increase of the DEM size in this study. The study by Yu (1997) also reported that a 183 m spacing

Table 7 Percentage deviation of the estimated soil loss from the observed sediment yield ($\text{Mg ha}^{-1} \text{ year}^{-1}$)

Year	30 m			50 m			100 m			150 m			200 m			250 m			Observed sediment yield	
	Cartosat	Aster	SRTM	Cartosat	Aster	SRTM	Cartosat	Aster	SRTM	Cartosat	Aster	SRTM	Cartosat	Aster	SRTM	Cartosat	Aster	SRTM	Aster	SRTM
1998	23.66	201.26	20.82	183.91	14.20	41.32	119.24	21.77	52.68	141.01	13.88	36.28	73.19	29.97	53.00	77.60	3.17	77.60	3.17	
1999	27.78	210.78	24.51	192.81	17.65	46.08	126.14	25.49	57.19	148.69	16.99	39.87	78.10	33.99	57.84	83.01	3.06	83.01	3.06	
2000	9.96	173.06	8.12	157.20	2.21	26.94	97.79	8.86	36.90	118.08	1.85	22.14	55.72	15.50	36.90	59.41	2.71	59.41	2.71	
2001	22.63	204.12	20.58	186.42	13.99	41.56	120.16	21.40	52.26	142.80	13.17	35.80	73.25	28.81	52.67	77.78	2.43	77.78	2.43	
Avg	21.01	197.31	18.51	180.08	12.01	38.98	115.83	19.38	49.76	137.65	11.47	33.52	70.07	27.07	50.10	74.45	2.84	74.45	2.84	

could be an appropriate compromise between the quality of hydrologic simulations and the amount of required computing time. Liu et al. (2009) evaluated the S factor's accuracy for different DEM resolutions and reported that the accuracy of the S factor decreases as the horizontal resolution decreases. Thus, coarse-resolution DEMs can be used in large river basins to avoid large memory data usage. Overall, the results suggested that the selection of DEM sources and grid sizes has a major influence on soil erosion estimation. Soil loss is most dependent on the flow path length. Thus, erosion modelling without considering the grid size or other lumping effects will drastically change the decisions concerning non-point source pollution control (Verstraeten, 2006). The reasons for the varied thresholds were due to the nonlinear nature of the erosion process (Chaplot 2005).

Variations in erosion estimates for multisource and multiresolution DEMs are attributed to the drainage network connectivity, which in turn influence the sediment transport capacity of the network. Furthermore, a satellite-based TRMM-gridded rainfall product facilitated the R factor's computation, which is a critical factor for understanding the hydrological and surface geomorphological processes at the watershed scale. Particularly, the availability of the total rainfall energy and maximum 30 min rainfall intensity (I_{30}) of storm events for the R factor's computation is rarely available in developing countries. Soil erosion assessments using the relationship between the annual rainfall and EI_{30} values proposed by Singh et al. (1981) for India's climatic regions yielded better results. One of the RUSLE model's major limitations is that it does not account for the transportation and deposition of the eroded sediments and provides only gross estimates of the soil erosion from the watershed. In the study area, the sediment transport efficiency is very high, considering the watershed and land-use/land-cover distribution, where more than 65% of the area is occupied by agriculture and non-forest classes. Furthermore, out of the 35% of the area covered by forest classes, only 2% is under dense forest, meaning that sediment's transport capacity is likely to be high. A well-distributed drainage network further aggregates the transport capacity of sediments. Hence, in this study, the concepts of either the sediment delivery ratio or transport-limited sediment delivery were not considered when assessing the soil erosion/deposition, as suggested in the literature (Jain and Kothari 2000). Higher agricultural areas, plantations, and degraded forests also reflect the various anthropogenic activities that increase the transport capacity (deVente et al. 2009). Thus, this study helped to assess the impact of the multisource and multiresolution DEMs on the erosion processes, which can be used when providing guidelines for the input data preparation requirements and computational resources needed for the

Fig. 6 **a** Spatial distribution of the average annual soil loss (ASTER), **b** spatial distribution of the average annual soil loss (Cartosat-1) and **c** spatial distribution of the average annual soil loss (SRTM)

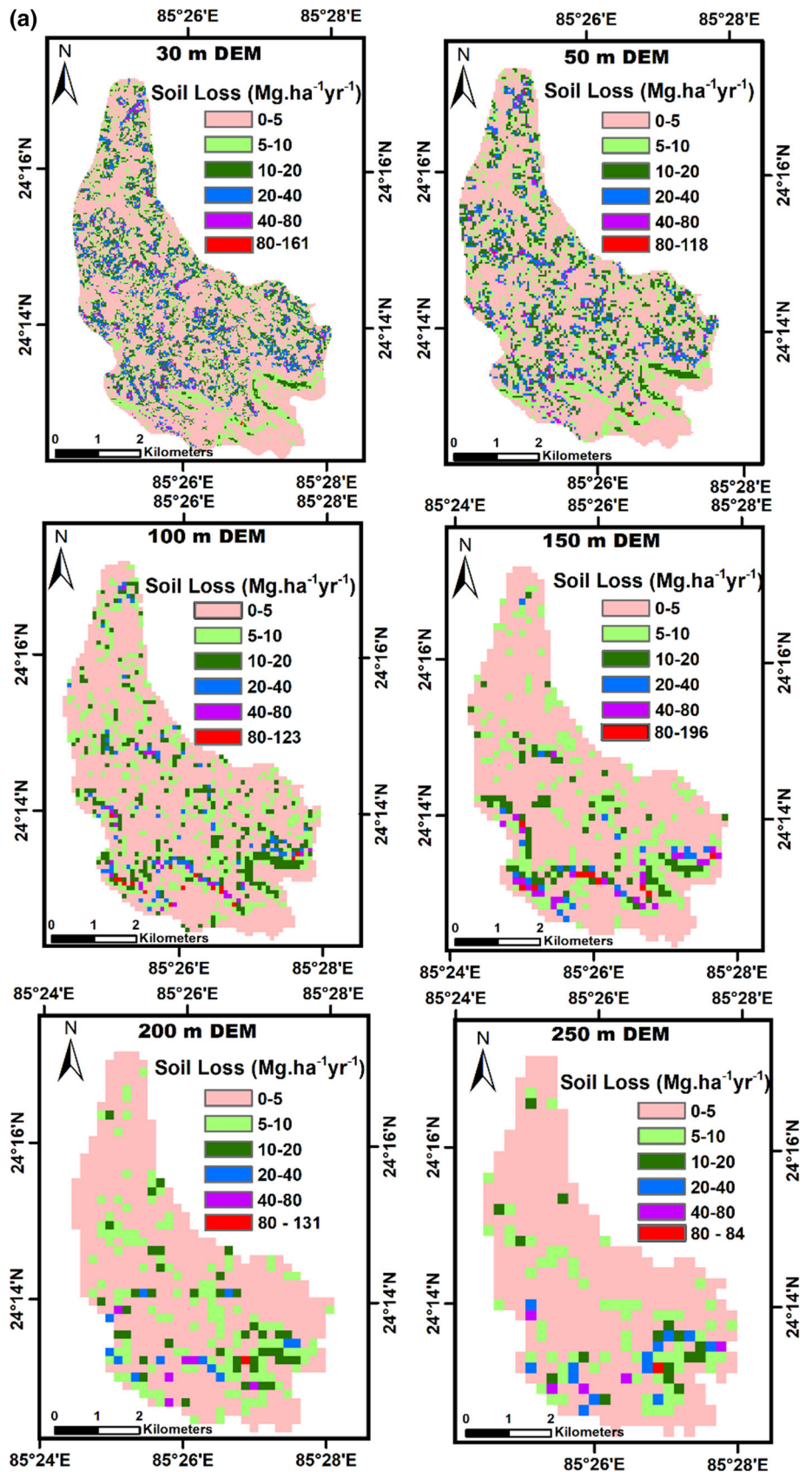


Fig. 6 continued

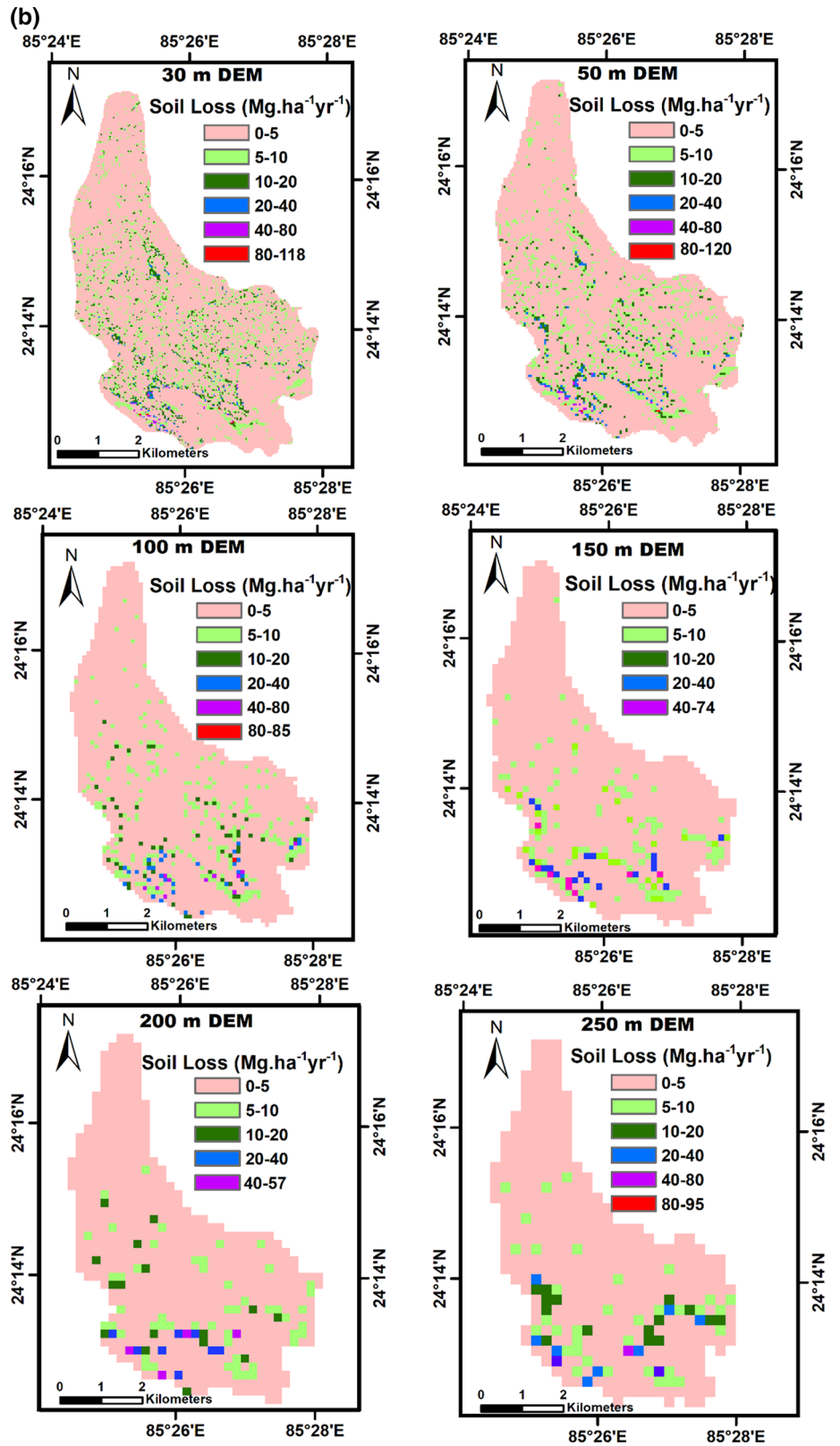
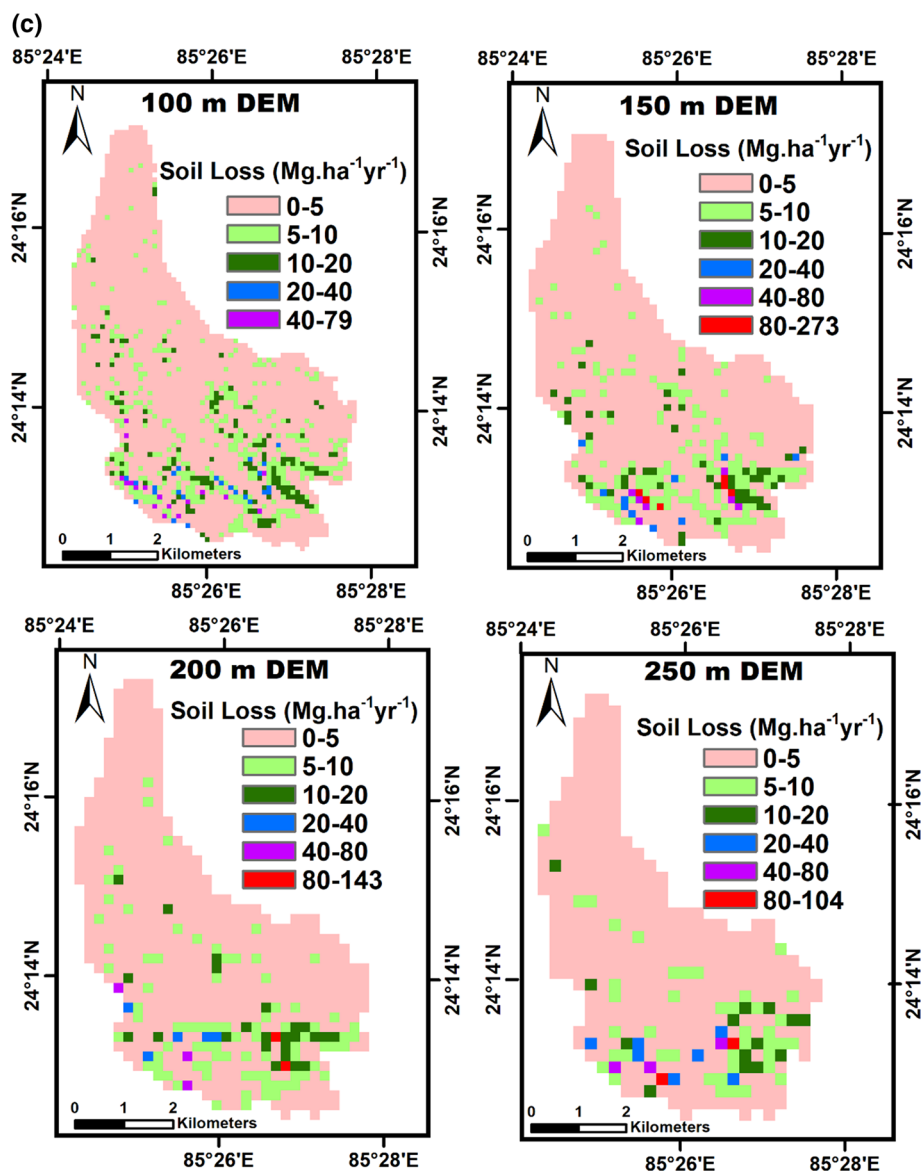


Fig. 6 continued



effective utilization of soil erosion models. Furthermore, accurate soil erosion estimation and its spatial distribution at the watershed, sub-watershed, and catchment scales are required to plan and effectively implement soil and water conservation interventions.

Conclusions

The study evaluated the effect of three DEMs, i.e., ASTER, Cartosat-1 and SRTM on erosion modelling over the Karso watershed using RUSLE and TRMM rainfall data. The TRMM-derived rainfall was used for the estimation of the *R* factor of the RUSLE model. Variations in the slope length factor were observed with a coarser resampled grid size, which consequently affected the soil loss estimate.

When estimating the soil loss using the RUSLE model, the Cartosat-DEM-derived parameters produced better results than the SRTM-DEM and ASTER-DEM derived parameters. The Cartosat-DEM at 100 m and 150 m appeared to be a threshold, where the RUSLE estimates for these grid resolutions matched reasonably well with the observed soil loss. In the SRTM-DEM case, the parameters derived using the 200 m resolution grid yielded better estimates compared to other grid resolutions. The ASTER DEM was found to be the poorest of all the tested DEMs. The results showed that the DEM source and grid size selection profoundly influenced soil loss estimation using the RUSLE model. The spatial distribution of the soil erosion in the watershed helps to identify cells that contribute to soil erosion and characterize the transport path. The present study was an effort to highlight the possible uncertainties

Table 8 Comparing the estimated soil losses ($\text{Mg ha}^{-1} \text{ year}^{-1}$) from different digital elevation models and grid sizes

Year	30 m		50 m		100 m		150 m		200 m		250 m	
	Cartosat	Aster	Cartosat	Aster	Cartosat	Aster	Cartosat	Aster	Cartosat	Aster	Cartosat	Aster
1998	3.92	9.55	3.83	9.00	3.62	4.48	3.86	4.84	3.61	4.32	4.12	4.85
1999	3.91	9.51	3.81	8.96	3.60	4.47	3.84	4.81	3.58	4.28	4.10	4.83
2000	2.98	7.40	2.93	6.97	2.77	3.44	2.95	3.71	2.76	3.31	3.13	3.71
2001	2.98	7.39	2.93	6.96	2.77	3.44	2.95	3.70	2.75	3.30	3.13	3.71
2002	2.85	7.12	2.79	6.70	2.65	3.30	2.82	3.55	2.63	3.16	3.00	3.55
2003	3.25	8.05	3.18	7.59	3.03	3.74	3.22	4.05	3.00	3.59	3.43	4.09
2004	2.99	7.42	2.94	6.99	2.78	3.45	2.96	3.72	2.76	3.32	3.13	3.73
2005	2.37	6.02	2.32	5.66	2.20	2.76	2.34	2.97	2.19	2.62	2.49	3.01
2006	3.51	8.63	3.44	8.14	3.26	4.04	3.46	4.38	3.24	3.87	3.67	4.39
2007	4.04	9.87	3.96	9.31	3.77	4.66	3.99	5.01	3.75	4.47	4.28	5.04
2008	3.44	8.47	3.38	7.99	3.18	3.95	3.40	4.28	3.18	3.79	3.61	4.29
2009	2.40	6.07	2.35	5.71	2.22	2.78	2.37	3.00	2.22	2.64	2.51	3.04
2010	2.41	6.11	2.37	5.75	2.24	2.79	2.39	3.02	2.23	2.66	2.52	3.06
2011	3.92	9.56	3.83	9.01	3.63	4.49	3.87	4.84	3.62	4.32	4.13	4.85
2012	3.16	7.81	3.09	7.35	2.93	3.63	3.12	3.93	2.93	3.49	3.29	3.93
Avg	3.21	7.93	3.14	7.47	2.98	3.69	3.17	3.99	2.96	3.54	3.37	4.01

associated with the use of multisource and multiresolution open-source DEMs during soil erosion modelling. The prediction of the erosion potential at the grid level using the RUSLE model helped to identify the soil erosion's spatial pattern within the watershed. Thus, assessment of the soil loss by RUSLE and multisource and multiresolution open-source DEMs helped to evaluate the effect of the topographic parameter on soil erosion processes.

Acknowledgments The hydrological data provided by Damodar Valley Corporation (DVC), Hazaribagh, India, and facilities provided by the Department of Water Resources Development and Management, IIT Roorkee, be highly appreciated.

Funding This research received no external funding.

References

- Ahmed, N., Mahtab, A., Agrawal, R., Jayaprasad, P., Pathan, S. K., Singh, D. K., & Singh, A. K. (2007). Extraction and validation of Cartosat-1 DEM. *Journal of the Indian Society of Remote Sensing*, 35, 121–127.
- Alcañiz, M., Úbeda, X., & Cerdà, A. (2020). A 13-year approach to understand the effect of prescribed fires and livestock grazing on soil chemical properties in Tivissa, NE Iberian Peninsula. *Forests*, 11(9), 1013.
- Angima, S. D., Stott, D. E., O'Neill, M. K., Ong, C. K., & Weesies, G. A. (2003). Soil erosion prediction using RUSLE for central Kenyan highland conditions. *Agriculture, Ecosystems and Environment*, 2003(97), 295–308.
- Barrow, C. J. (1991). *Land degradation*. Cambridge: Cambridge University Press.
- Cerdà, A., Borja, M. E. L., Úbeda, X., Martínez-Murillo, J. F., & Keesstra, S. (2017). *Pinus halepensis* M. versus *Quercus ilex* subsp. *Rotundifolia* L. runoff and soil erosion at pedon scale under natural rainfall in Eastern Spain three decades after a forest fire. *Forest Ecology and Management*, 400, 447–456.
- Cerdà, A., Rodrigo-Comino, J., Yakupoğlu, T., Dindaroğlu, T., Terol, E., Mora-Navarro, G., et al. (2020). Tillage versus no-tillage. Soil properties and hydrology in an organic persimmon farm in Eastern Iberian Peninsula. *Water*, 12(6), 1539.
- Chaplot, V. (2005). Impact of DEM mesh size and soil map scale on SWAT runoff, sediment, and NO₃-N loads predictions. *Journal of Hydrology*, 312, 207–222.
- Chaubey, I., Cotter, A. S., Costello, T. A., & Soerens, T. S. (2005). Effect of DEM data resolution on SWAT output uncertainty. *Hydrological Processes*, 19, 621–628.
- Chen, T., Niu, R. Q., Li, P. X., Zhang, L. P., & Du, B. (2011). Regional soil erosion risk mapping using RUSLE, GIS, and remote sensing: A case study in Miyun watershed, North China. *Environmental Earth Sciences*, 63, 533–541.
- Cho, S. M., & Lee, M. (2001). Sensitivity considerations when modeling hydrologic processes with digital elevation model. *The Journal of the American Water Resources Association*, 37, 931–934.
- Cochrane, T. A., & Flanagan, D. C. (2005). Effect of DEM resolutions in the runoff and soil loss predictions of the WEPP watershed model. *Transaction on ASAE*, 2005(48), 109–120.
- Cohen, J. (1968). Weighted kappa: Nominal scale agreement provision for scaled disagreement or partial credit. *Psychological Bulletin*, 70, 213.
- Cohen, M. J., Shepherd, K. D., & Walsh, M. G. (2005). Empirical formulation of the universal soil loss equation for erosion risk assessment in a tropical watershed. *Geoderma*, 2005(124), 235–252.
- Collischonn, B., Collischonn, W., & Tucci, C. E. M. (2008). Daily hydrological modeling in the Amazon basin using TRMM rainfall estimates. *Journal of Hydrology*, 360, 207–216.
- Cotter, A. S., Chaubey, I., Costello, T. A., Soerens, T. S., & Nelson, M. A. (2003). Water quality model output uncertainty as affected by spatial resolution of input data. *The Journal of the American Water Resources Association*, 39, 977–986.
- Dabral, P. P., Baithuri, N., & Pandey, A. (2008). Soil erosion assessment in a hilly catchment of North Eastern India using USLE, GIS and remote sensing. *Water Resources Management*, 22, 1783–1798.
- Datta, P., & Schack-Kirchner, H. (2010). Erosion relevant topographical parameters derived from different DEMs—A comparative study from the Indian Lesser Himalayas. *Remote Sensing*, 2, 1941–1961.
- Demirci, A., & Karaburun, A. (2012). Estimation of soil erosion using RUSLE in a GIS framework: A case study in the Buyukcekmece Lake watershed, northwest Turkey. *Environmental Earth Sciences*, 66, 903–913.
- deVente, J., Poesen, J., Govers, G., & Boix-Fayos, C. (2009). The implications of data selection for regional erosion and sediment yield modelling. *Earth Surface Processes and Landforms*, 34, 1994–2007.
- Di Luzio, M., Srinivasan, R., & Arnold, J. G. (2004). A GIS-coupled hydrological model system for the watershed assessment of agricultural nonpoint and point sources of pollution. *Transaction in GIS*, 8, 113–136.
- Diodato, N., & Bellocchi, G. (2007). Estimating monthly (R) USLE climate input in a mediterranean region using limited data. *Journal of Hydrology*, 345, 224–236.
- Duncan, J., & Biggs, E. M. (2012). Assessing the accuracy and applied use of satellite-derived precipitation estimates over Nepal. *Applied Geography*, 34, 626–638.
- Fistikoglu, O., & Harmancioglu, N. B. (2002). Integration of GIS with USLE in assessment of soil erosion. *Water Resources Management*, 16, 447–467.
- Fujisada, H., Bailey, G. B., Kelly, G. G., Hara, S., & Abrams, M. J. (2005). Aster dem performance. *IEEE Transactions on Geoscience and Remote Sensing*, 43(12), 2707–2714.
- Ghosal, K., & Bhattacharya, S. D. (2020). A Review of RUSLE model. *Journal of the Indian Society of Remote Sensing*, 48, 689–707.
- Hancock, G. R., Martinez, C., Evans, K. G., & Moliere, D. R. (2006). A comparison of SRTM and high-resolution digital elevation models and their use in catchment geomorphology and hydrology: Australian examples. *Earth Surface Processes and Landforms*, 31, 1394–1412.
- Hayakawa, Y. S., Oguchi, T., & Lin, Z. (2008). Comparison of new and existing global digital elevation models ASTER G-DEM and SRTM-3. *Geophysical Research Letters*, 35, L17404.
- Hirt, C., Filmer, M. S., & Featherstone, W. E. (2010). Comparison and validation of the recent freely available ASTER-GDEM ver1, SRTM ver4. 1 and GEODATA DEM-9S ver3 digital elevation models over Australia. *Australian Journal of Earth Sciences*, 57, 337–347.
- Islam, M. N., & Uyeda, H. (2007). Use of TRMM in determining the climatic characteristics of rainfall over Bangladesh. *Remote Sensing of Environment*, 108, 264–276.
- Jain, M. K., & Kothyari, U. C. (2000). Estimation of soil erosion and sediment yield using GIS. *Hydrological Sciences Journal*, 45, 771–786.

- Kääb, A. (2005). Combination of SRTM3 and repeat ASTER data for deriving alpine glacier flow velocities in the Bhutan Himalaya. *Remote Sensing of Environment*, 94, 463–474.
- Karaseva, M. O., Prakash, S., & Gairola, R. M. (2011). Validation of high-resolution TRMM-3B43 precipitation product using rain gauge measurements over Kyrgyzstan. *Theoretical and Applied Climatology*, 108, 147–157.
- Katiraei-Boroujerdy, P. S., Nasrollahi, N., Hsu, K. L., & Sorooshian, S. (2013). Evaluation of satellite-based precipitation estimation over Iran. *Journal of Arid Environments*, 97, 205–219.
- Keesstra, S., Mol, G., de Leeuw, J., Okx, J., de Cleen, M., & Visser, S. (2018). Soil-related sustainable development goals Four concepts to make land degradation neutrality and restoration work. *Land*, 7, 133.
- Keesstra, S., Nunes, J. P., Saco, P., Parsons, T., Poepl, R., Masselink, R., & Cerdà, A. (2018a). The way forward: Can connectivity be useful to design better measuring and modelling schemes for water and sediment dynamics? *Science of the Total Environment*, 644, 1557–1572.
- Keesstra, S. D., Rodrigo-Comino, J., Novara, A., Giménez-Morera, A., Pulido, M., Di Prima, S., & Cerdà, A. (2019). Straw mulch as a sustainable solution to decrease runoff and erosion in glyphosate-treated clementine plantations in Eastern Spain. An assessment using rainfall simulation experiments. *CATENA*, 174, 95–103.
- Kummerow, C., Barnes, W., Kozu, T., Shiue, J., & Simpson, J. (1998). The tropical rainfall measuring mission (TRMM) sensor package. *The Journal of Atmospheric and Oceanic Technology*, 15, 809–817.
- Li, J., & Wong, D. W. S. (2010). Effects of DEM sources on hydrologic applications. *Computers, Environment and Urban Systems*, 34, 251–261.
- Lin, S., Jing, C., Chaplot, V., Yu, X., Zhang, Z., Moore, N., & Wu, J. (2010). Effect of DEM resolution on SWAT outputs of runoff, sediment and nutrients. *Hydrology and Earth System Sciences Discussions*, 7, 4411–4435.
- Lin, S., Jing, C., Coles, N. A., Chaplot, V., Moore, N. J., & Wu, J. (2013). Evaluating DEM source and resolution uncertainties in the soil and water assessment tool. *Stochastic Environmental Research and Risk Assessment*, 27, 209–221.
- Liu, X., Zhang, S., Zhang, X., Ding, G., & Cruse, R. M. (2009). Soil erosion control practices in Northeast China: A mini-review. *Soil and Tillage Research*, 117, 44–48.
- López-Vicente, M., Calvo-Seas, E., Álvarez, S., & Cerdà, A. (2020). Effectiveness of cover crops to reduce loss of soil organic matter in a Rainfed vineyard. *Land*, 9, 230.
- Molnár, D. K., & Julien, P. Y. (1998). Estimation of upland erosion using GIS. *Computers and Geosciences*, 24, 183–192.
- Mondal, A., Khare, D., & Kundu, S. (2017). Uncertainty analysis of soil erosion modelling using different resolution of open-source DEMs. *Geocarto International*, 32, 334–349.
- Moore, I., & Burch, G. (1986). Physical basis of the length-slope factor in the universal soil loss equation. *Soil Science Society of America Journal*, 50, 1294–1298.
- Mukherjee, S., Joshi, P. K., Mukherjee, S., Ghosh, A., Garg, R. D., & Mukhopadhyay, A. (2013). Evaluation of vertical accuracy of open source Digital Elevation Model (DEM). *International Journal of Applied Earth Observation and Geoinformation*, 21, 205–217.
- Muralikrishnan, S., Pillai, A., Narender, B., Reddy, S., Venkataraman, V. R., & Dadhwal, V. K. (2013). Validation of Indian national DEM from Cartosat-1 data. *Journal of the Indian Society of Remote Sensing*, 41, 1–13.
- Murthy, Y. N. K., Rao, S. S., Rao, D. S., & Jayaraman, V. (2008). Analysis of DEM generated using Cartosat-1 stereo data over Mausanne Les alpines-Cartyosat—Scientific appraisal programme (CSAP TS-5). *The International Archives of the Photogrammetry, Remote Sensing and Spatial Information Sciences*, 37, 1343–1348.
- Narayana, D. V., & Babu, R. (1983). Estimation of soil erosion in India. *Journal of Irrigation and Drainage Engineering*, 109, 419–434.
- Nikolakopoulos, K. G., Kamaratakis, E. K., & Chrysoulakis, N. (2006). SRTM vs ASTER elevation products. Comparison for two regions in Crete, Greece. *International Journal of Remote Sensing*, 27, 4819–4838.
- Novara, A., Stallone, G., Cerdà, A., & Gristina, L. (2019). The effect of shallow tillage on soil erosion in a semi-arid vineyard. *Agronomy*, 9(5), 257.
- Onyando, J. O., Kisoyan, P., & Chemelil, M. C. (2005). Estimation of potential soil erosion for river perkerra catchment in Kenya. *Water Resources Management* 19, 133–143.
- Pandey, A., Chowdary, V. M., & Mal, B. C. (2007). Identification of critical erosion prone areas in the small agricultural watershed using USLE, GIS and remote sensing. *Water Resources Management*, 21, 729–746.
- Pandey, A., Chowdary, V. M., Mal, B. C., & Billib, M. (2008). Runoff and sediment yield modeling from a small agricultural watershed in India using the WEPP model. *Journal of Hydrology*, 348, 305–319.
- Pandey, A., Mathur, A., Mishra, S. K., & Mal, B. C. (2009). Soil erosion modeling of a Himalayan watershed using RS and GIS. *Environmental Earth Sciences*, 59, 399–410.
- Prasuhn, V., Liniger, H., Gisler, S., Herweg, K., Candinas, A., & Clément, J. P. (2013). A high-resolution soil erosion risk map of Switzerland as strategic policy support system. *Land Use Policy*, 32, 281–291.
- Quiquerez, A., Chevigny, E., Allemand, P., Curmi, P., Petit, C., & Grandjean, P. (2014). Assessing the impact of soil surface characteristics on vineyard erosion from very high spatial resolution aerial images (Côte de Beaune, Burgundy, France). *CATENA*, 116, 163–172.
- Rabus, B., Eineder, M., Roth, A., & Bamler, R. (2003). The shuttle radar topography mission—A new class of digital elevation models acquired by spaceborne radar. *ISPRS Journal of Photogrammetry and Remote Sensing*, 57, 241–262.
- Rao, Y. P. (1981). Evaluation of cropping management factor in universal soil loss equation under natural rainfall condition of Kharagpur, India. In *Proceedings of Southeast Asian regional symposium on problems of soil erosion and sedimentation. Asian Institute of Technology, Bangkok, Thailand* (pp. 241–254).
- Renard, K. G., Foster, G. R., Weesies, G. A., McCool, D. K., & Yoder, C. (1997). Predicting soil erosion by water: A guide to conservation planning with the revised universal soil loss equation (RUSLE). *Handbook of Agriculture*, 703, 1–367.
- Renschler, C. S., & Harbor, J. (2002). Soil erosion assessment tools from point to regional scales the role of geomorphologists in land management research and implementation. *Geomorphology*, 47, 189–209.
- Rodrigo-Comino, J. (2018). Five decades of soil erosion research in “terroir”. The State-of-the-Art. *Earth-Science Reviews*, 179, 436–447.
- Rodrigo-Comino, J., Giménez-Morera, A., Panagos, P., Pourghasemi, H. R., Pulido, M., & Cerdà, A. (2020). The potential of straw mulch as a nature-based solution for soil erosion in olive plantation treated with glyphosate: A biophysical and socio-economic assessment. *Land Degradation and Development*, 31, 1877–1889.
- Rodrigo-Comino, J., Keesstra, S., & Cerdà, A. (2018). Soil erosion as an environmental concern in vineyards: the case study of Celler del Roure, Eastern Spain, by means of rainfall simulation experiments. *Beverages*, 4(2), 31.

- Shamshad, A., Azhari, M. N., Isa, M. H., WanHussin, W. M. A., & Parida, B. P. (2008). Development of an appropriate procedure for estimation of RUSLEEI30 index and preparation of erosivity maps for Pulau Penang in Peninsular Malaysia. *CATENA*, 72, 423–432.
- Sharma, A., Tiwari, K. N., & Bhadoria, P. B. S. (2011). Determining the optimum cell size of digital elevation model for hydrologic application. *Journal of Earth System Science*, 120, 573–582.
- Singh, G., Chandra, S., & Babu, R. (1981). *Soil loss and prediction research in India*. New York: Central Soil and Water Conservation Research Training Institute.
- Thomas, J., Joseph, S., & Thrivikramji, K. P. (2018). Assessment of soil erosion in a tropical mountain river basin of the southern Western Ghats, India using RUSLE and GIS. *Geoscience Frontiers*, 9, 893–906.
- Van Oost, K., Govers, G., & Desmet, P. J. J. (2000). Evaluating the effects of changes in landscape structure on soil erosion by water and tillage. *Landscape Ecology*, 15, 577–589.
- Van Rompaey, A. J. J., Verstraeten, G., van Oost, K., Govers, G., & Poesen, J. (2001). Modelling mean annual sediment yield using a distributed approach. *Earth Surface Processes and Landforms*, 26, 1221–1236.
- Verstraeten, G. (2006). Regional scale modelling of hillslope sediment delivery with SRTM elevation data. *Geomorphology*, 81, 128–140.
- Vieux, B. F., & Needham, S. (1993). Nonpoint pollution model sensitivity to grid cell size. *Journal of Water Resources Planning and Management*, 119, 141–157.
- Vrieling, A., De Jong, S. M., Sterk, G., & Rodrigues, S. C. (2008). Timing of erosion and satellite data: A multi-resolution approach to soil erosion risk mapping. *International Journal of Applied Earth Observation and Geoinformation*, 10, 267–281.
- Vrieling, A., Sterk, G., & de Jong, S. M. (2010). Satellite-based estimation of rainfall erosivity for Africa. *Journal of Hydrology*, 395, 235–241.
- Walker, J. P., & Willgoose, G. R. (1999). On the effect of digital elevation model accuracy on hydrology and geomorphology. *Water Resources Research*, 35, 2259–2268.
- Wechsler, S. P. (2007). Uncertainties associated with digital elevation models for hydrologic applications: A review. *Hydrology and Earth System Sciences Discussions*, 11, 1481–1500.
- Wu, S., Li, J., & Huang, G. (2005). An evaluation of grid size uncertainty in empirical soil loss modeling with digital elevation models. *Environmental Modeling and Assessment*, 10, 33–42.
- Wuepper, D., Borrelli, P., & Finger, R. (2020). Countries and the global rate of soil erosion. *Nature Sustainability*, 3(1), 51–55.
- Yamaguchi, Y., Kahle, A. B., Tsu, H., Kawakami, T., & Pniel, M. (1998). Overview of advanced spaceborne thermal emission and reflection radiometer (ASTER). *Geoscience and Remote Sensing*, 36, 1062–1071.
- Yu, Z. (1997). Grid-spacing effect on watershed hydrologic simulations. *Hydrological Science and Technology*, 1997(13), 75–86.
- Zhang, J. X., Chang, K. T., & Wu, J. Q. (2008). Effects of DEM resolution and source on soil erosion modelling: A case study using the WEPP model. *International Journal of Geographical Information Science*, 22, 925–942.

Publisher's Note Springer Nature remains neutral with regard to jurisdictional claims in published maps and institutional affiliations.